

Supporting Information

Tunable and Stable White Light Emission in Bi³⁺ Alloyed Cs₂AgInCl₆ Double Perovskite Nanocrystals

*Debjit Manna, Tapan Kumar Das, Aswani Yella**

Department of Metallurgical Engineering & Materials Science, Indian Institute of Technology
Bombay, Powai, Mumbai, India-400076

* email: aswani.yella@iitb.ac.in

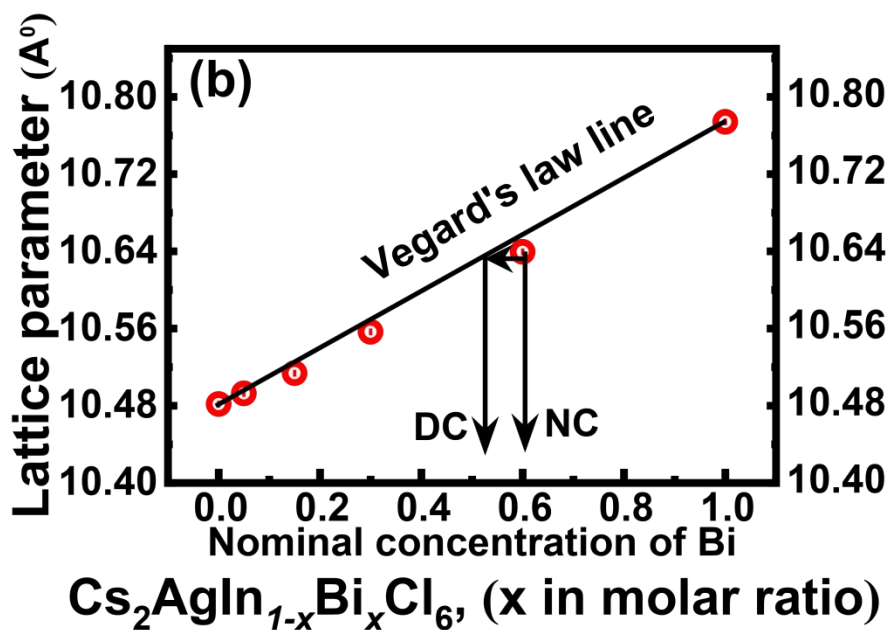
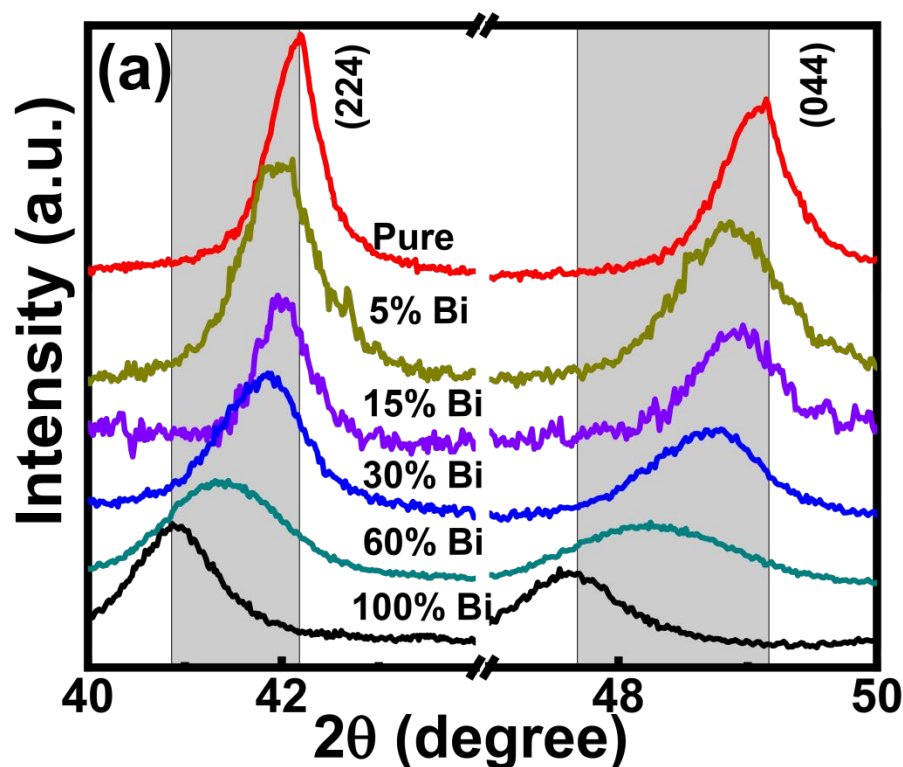


Figure S1. (a) XRD pattern showing of a zoomed portion of the reflection (224) and (004) planes of $\text{Cs}_2\text{AgIn}_{1-x}\text{Bi}_x\text{Cl}_6$ double perovskite with different doping concentration of Bi. This shows a systematic shift of angle 2θ with function of doping concentration; (b) Shows the variation of lattice parameter as a function of Bi doping. The black line connection between the lattice parameter of $\text{Cs}_2\text{AgInCl}_6$ and $\text{Cs}_2\text{AgBiCl}_6$ the theoretical Vegard's law line. The doping concentrations are estimated from the nominal concentration using Vegard's law line.

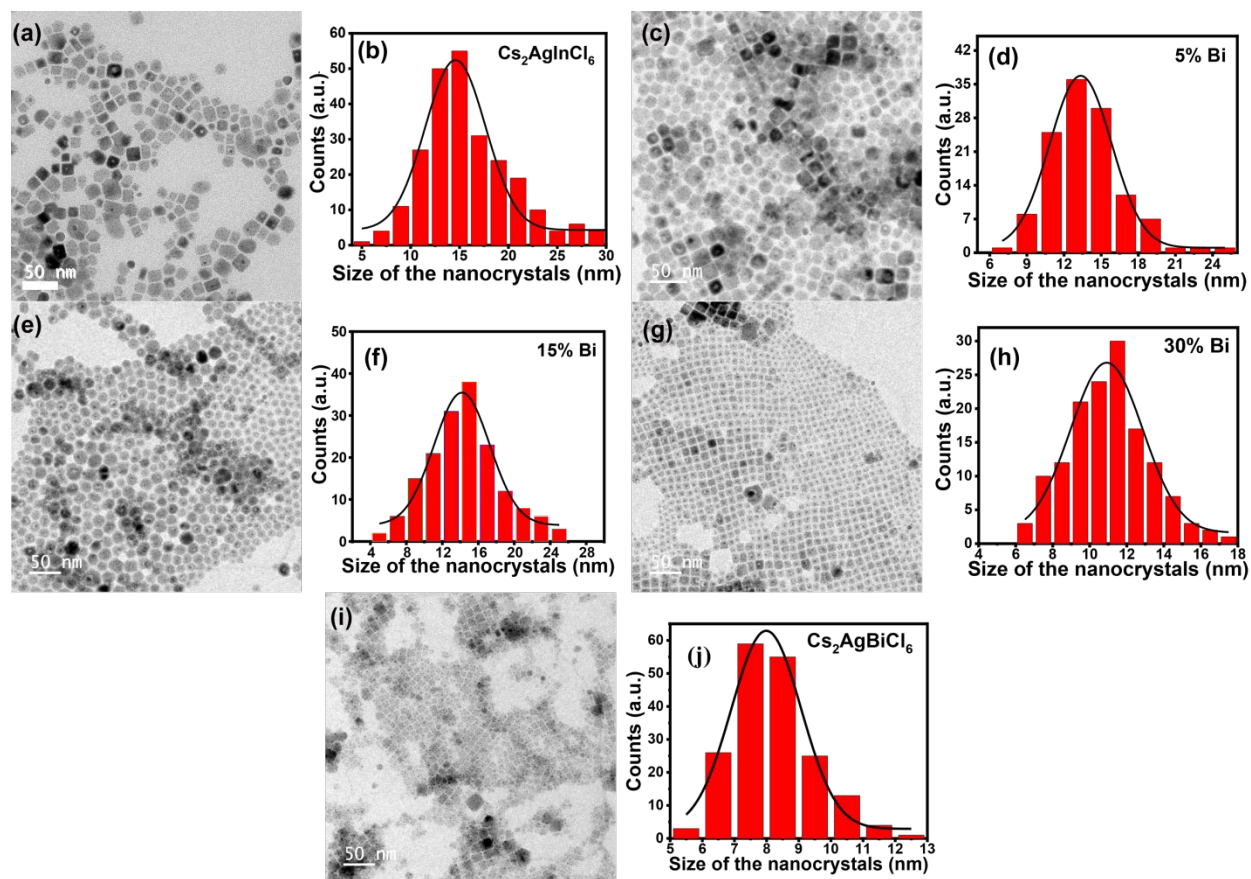


Figure S2. Size distribution estimated from TEM image of $\text{Cs}_2\text{AgIn}_{1-x}\text{Bi}_x\text{Cl}_6$ for (a,b) $x=0$; (c,d) $x=0.05$; (e, f) $x=0.15$; (g, h) $x=0.3$; (i, j) $x=1$ double perovskite nanocrystals. This distribution was done using Image J software by taking a greater number of selected low magnification TEM images.

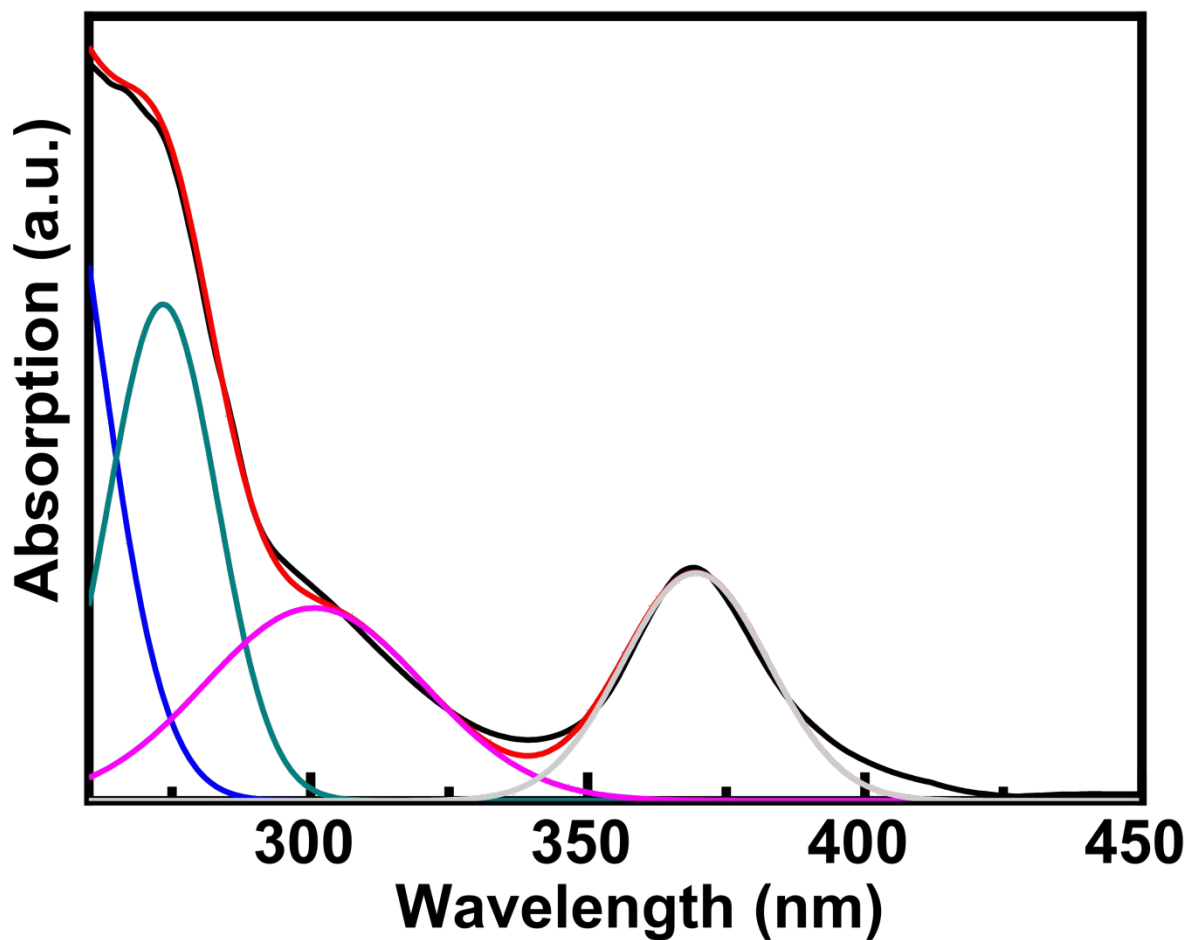


Figure S3. Peak fitting of UV-Visible absorption spectra of one representative sample. This fitting was used to calculate the integrated area under the first excitonic peak to calculate the oscillator strength.

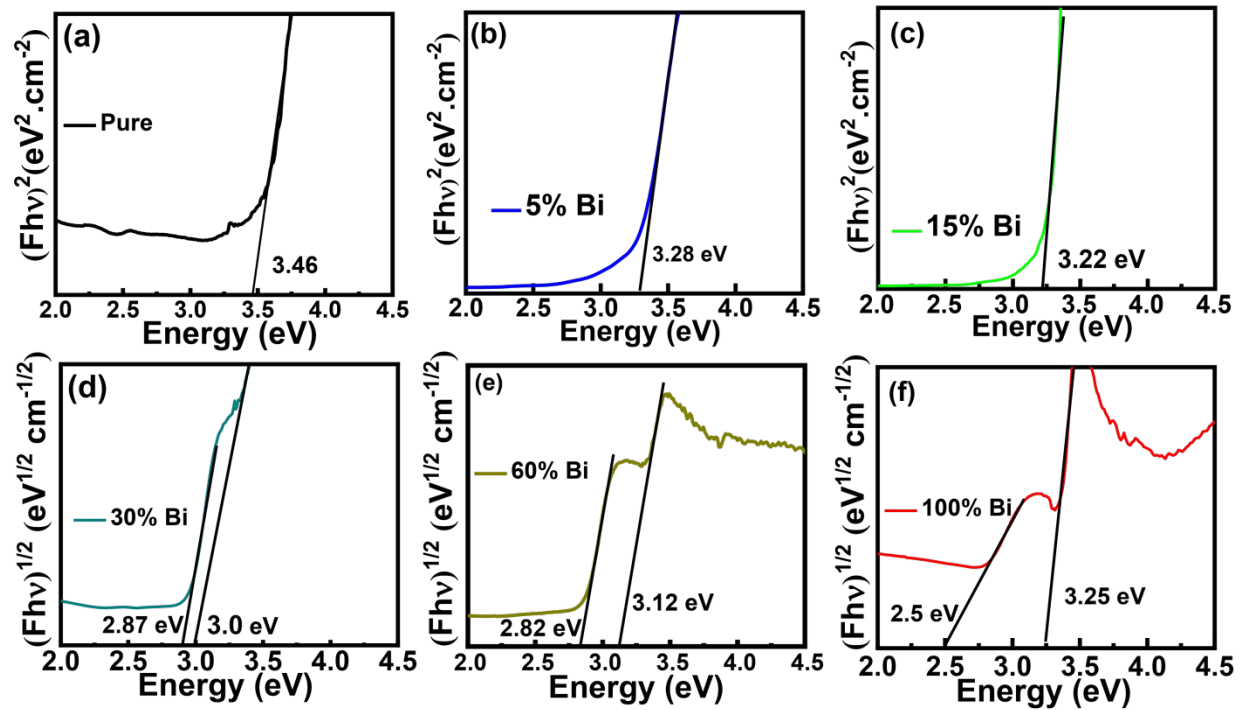


Figure S4. Tauc plot for $\text{Cs}_2\text{AgIn}_{1-x}\text{Bi}_x\text{Cl}_6$ with different Bi doping concentration for direct band (top panel) and indirect band (bottom panel) from the diffuse reflectance spectra (DRS). The spectra were collected with respect to standard BaSO_4 thin film in integrating sphere configuration.

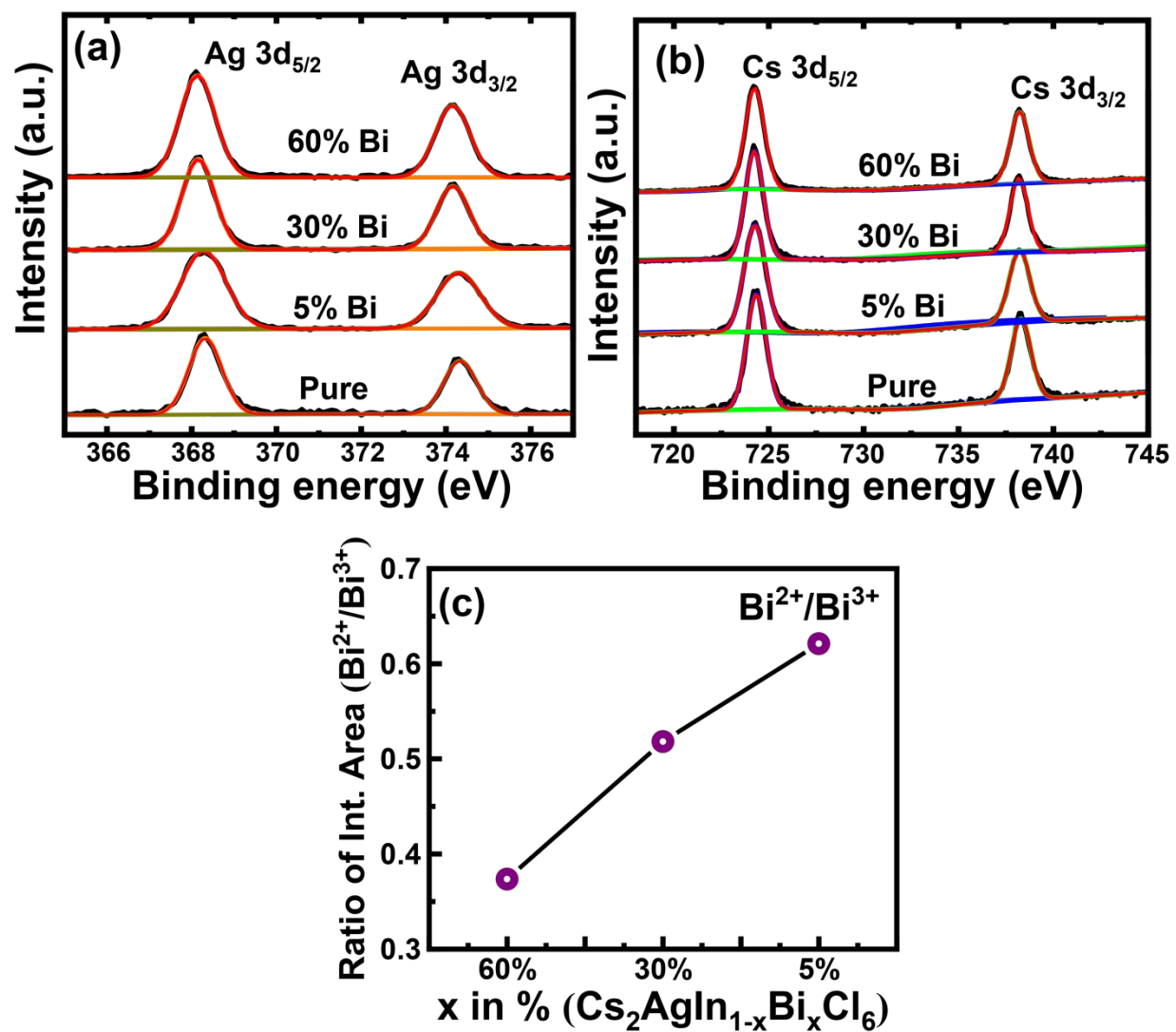


Figure S5. XPS spectra of (a) ‘Ag-3d’; (b) ‘Cs-3d’ in Cs₂AgIn_{1-x}Bi_xCl₆ with different Bi doping concentration (where x= 0, 0.05, 0.30 and 0.60); (c) The ratio of the integrated area of Bi²⁺/Bi³⁺ estimated from the peak fit of Bi 4f_{7/2}.

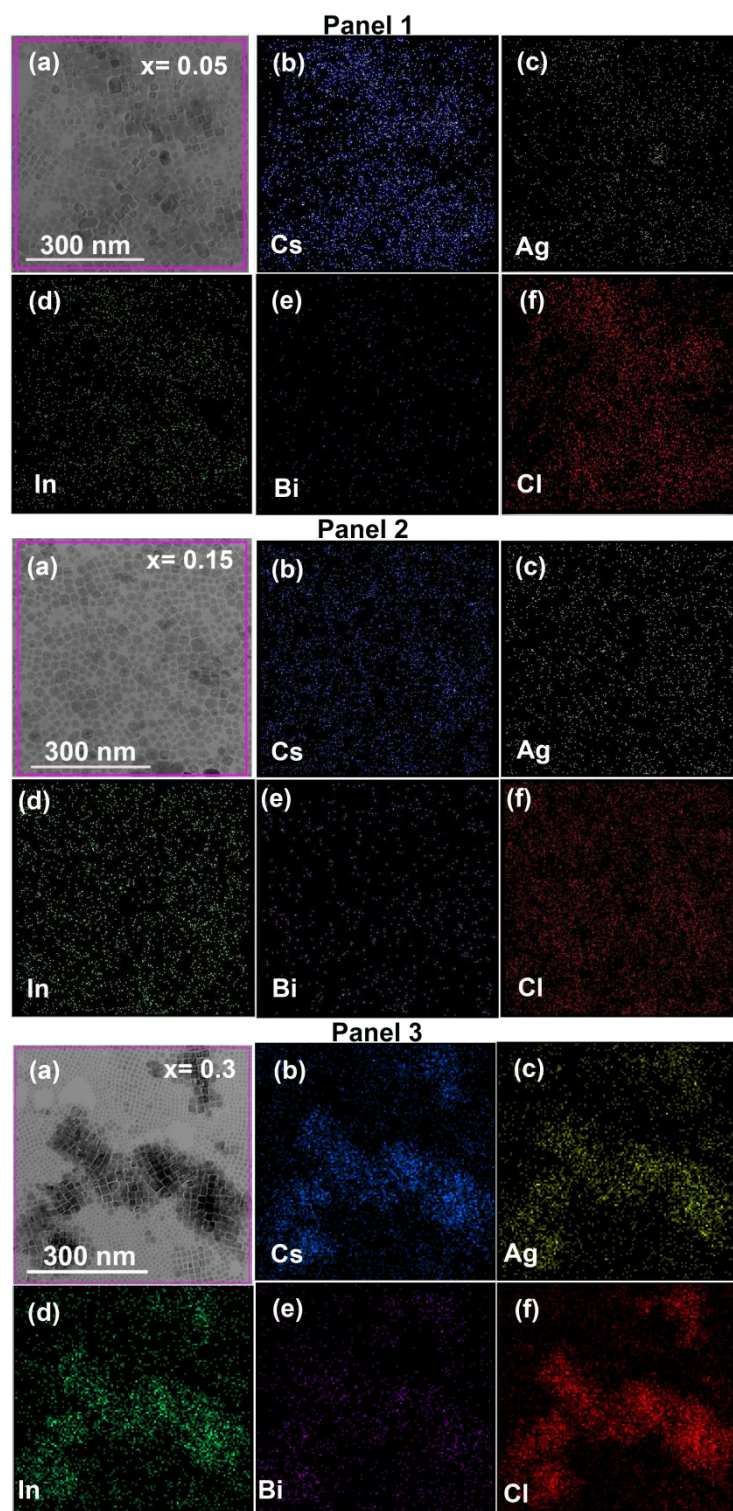


Figure S6. STEM-EDS mapping of some representative samples. Panel 1, 5% Bi doped; Panel 2, 15% Bi doped and Panel 3, 30% Bi doped Cs₂AgInCl₆ double perovskites respectively. All the measured compositions are given in the Table S3 and the EDS spectra are shown in Figure S7.

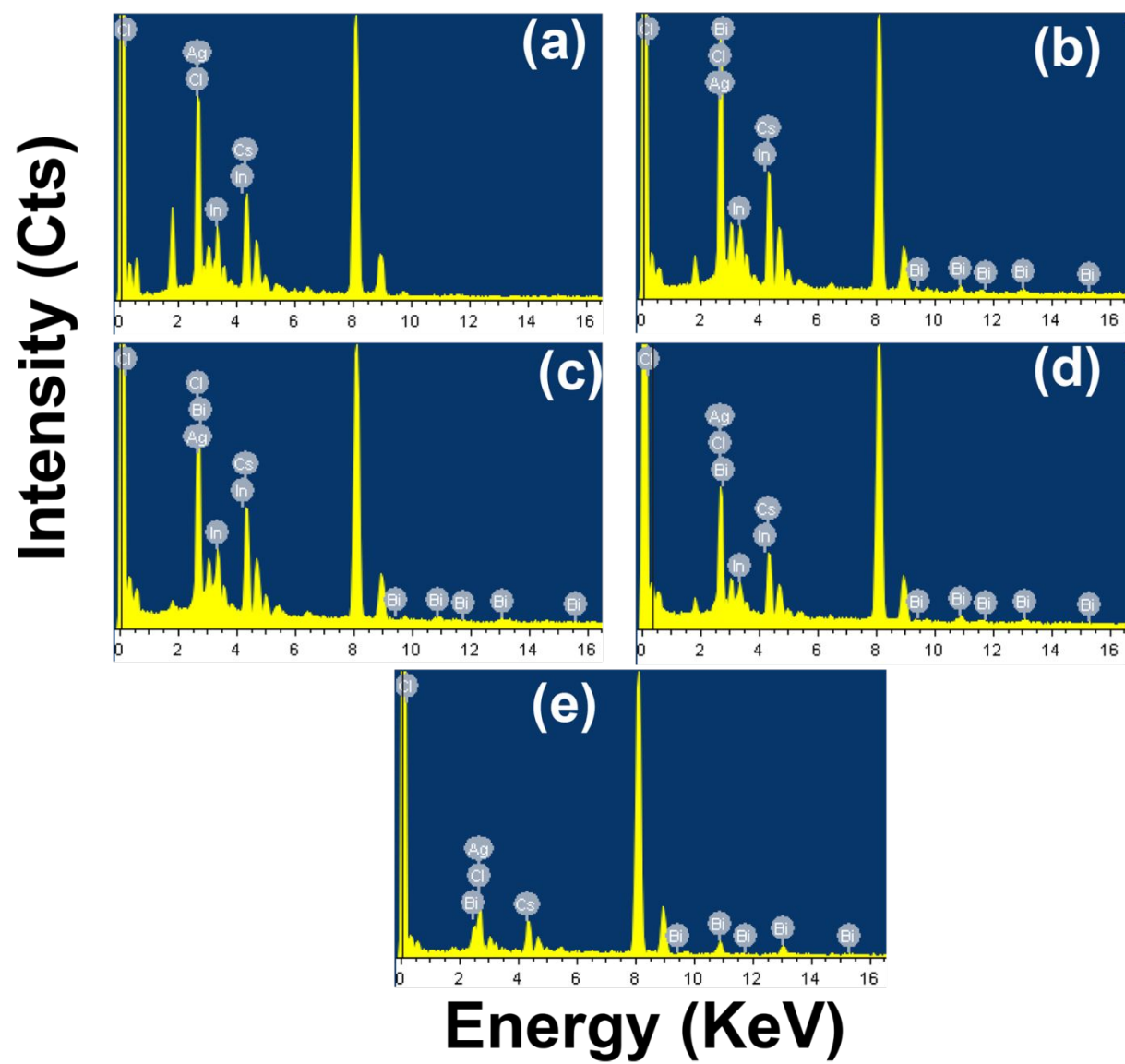


Figure S7. STEM-EDS spectra of $\text{Cs}_2\text{AgIn}_{1-x}\text{Bi}_x\text{Cl}_6$ double perovskite nanocrystals with, (a) $x=0$, (b) $x=5\%$, (c) $x=15\%$, (d) $x=30\%$, (e) $x=100\%$ of different concentration of Bi doping.

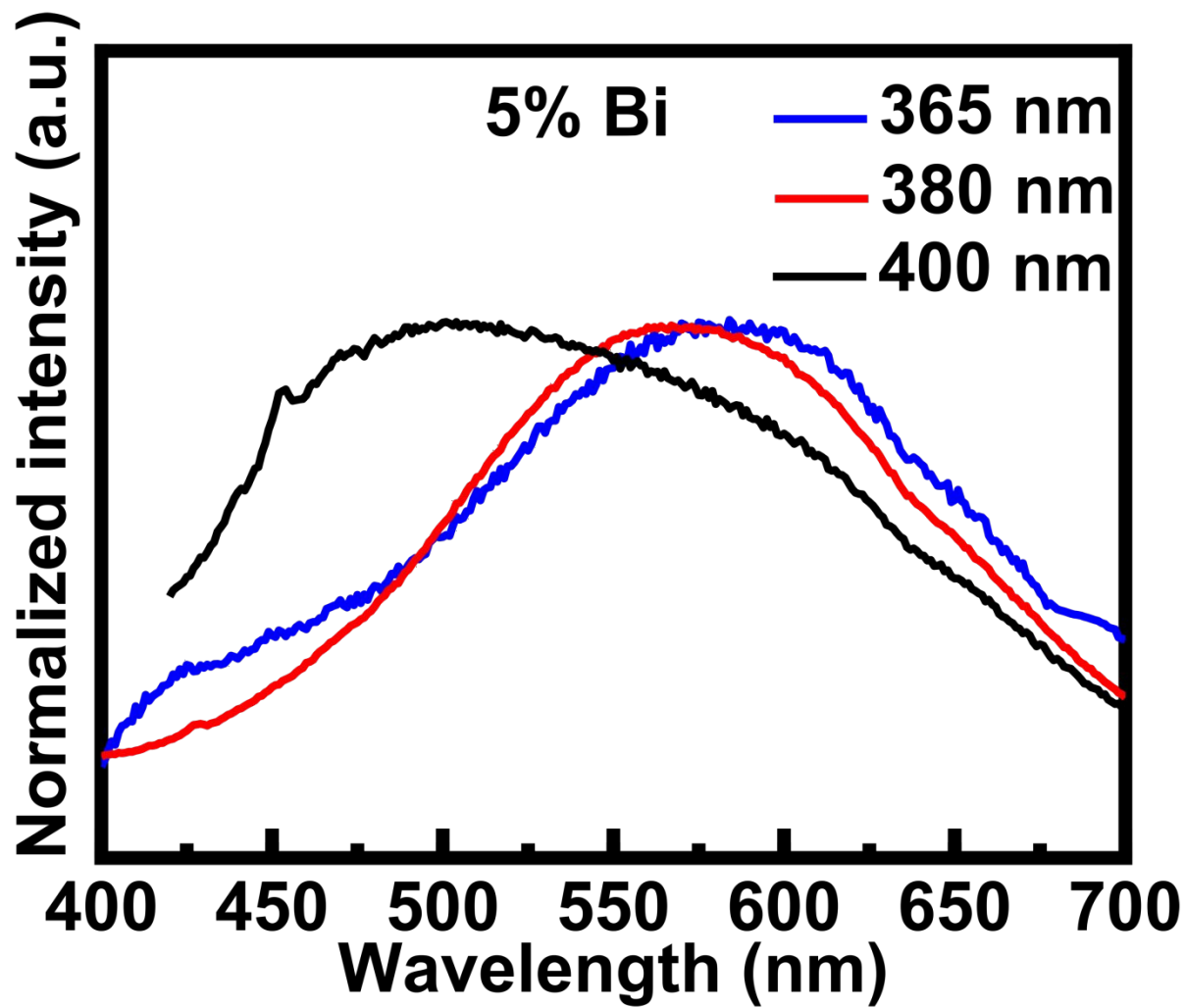


Figure S8. The PL spectra of 5% Bi doped in $\text{Cs}_2\text{AgInCl}_6$ nanocrystals collected at different excitation wavelength.

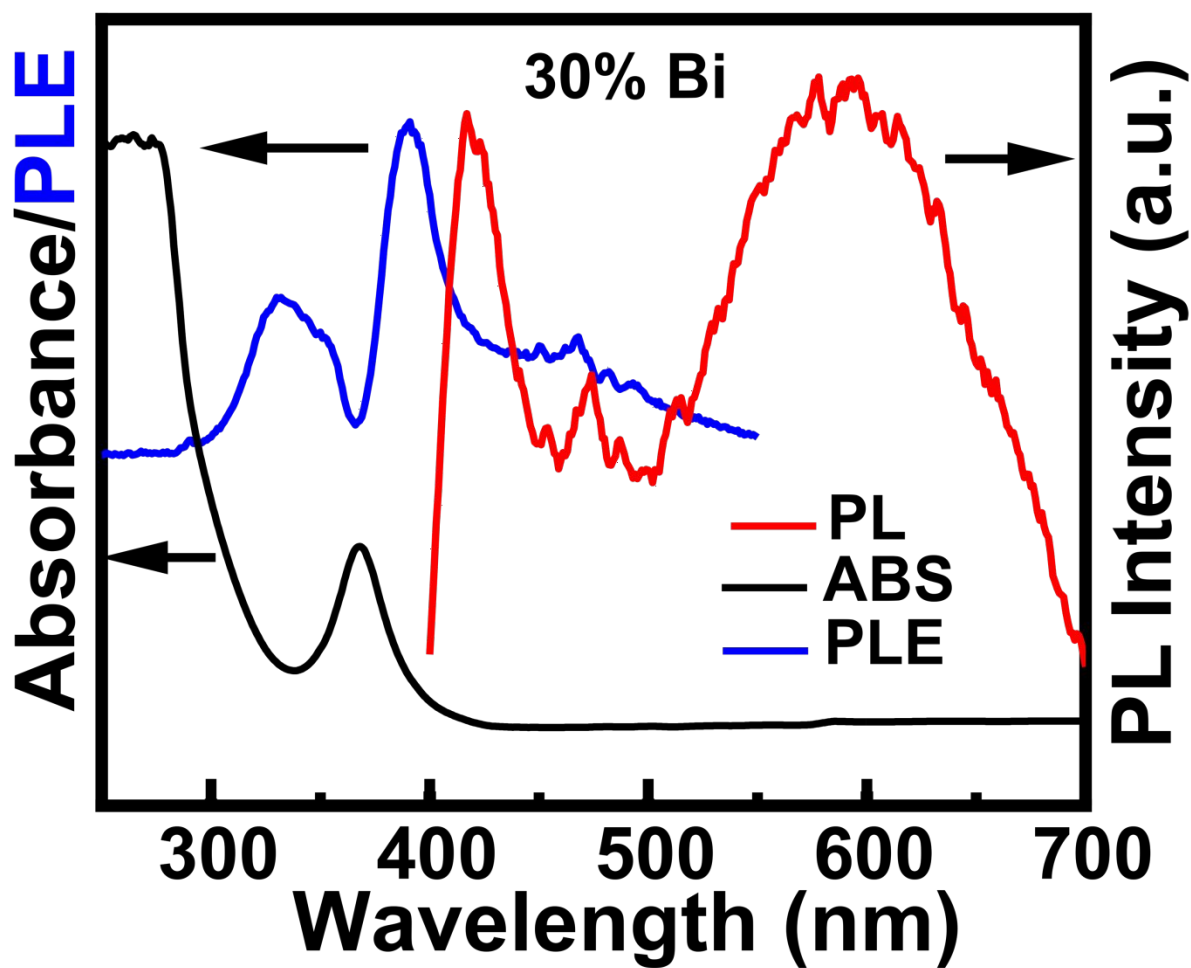


Figure S9. UV-Visible absorption (black line), PLE (emission at 580 nm, blue line) and PL (excitation at 380 nm, red line) of 30% Bi doped in $\text{Cs}_2\text{AgInCl}_6$ nanocrystals dispersed in hexane.

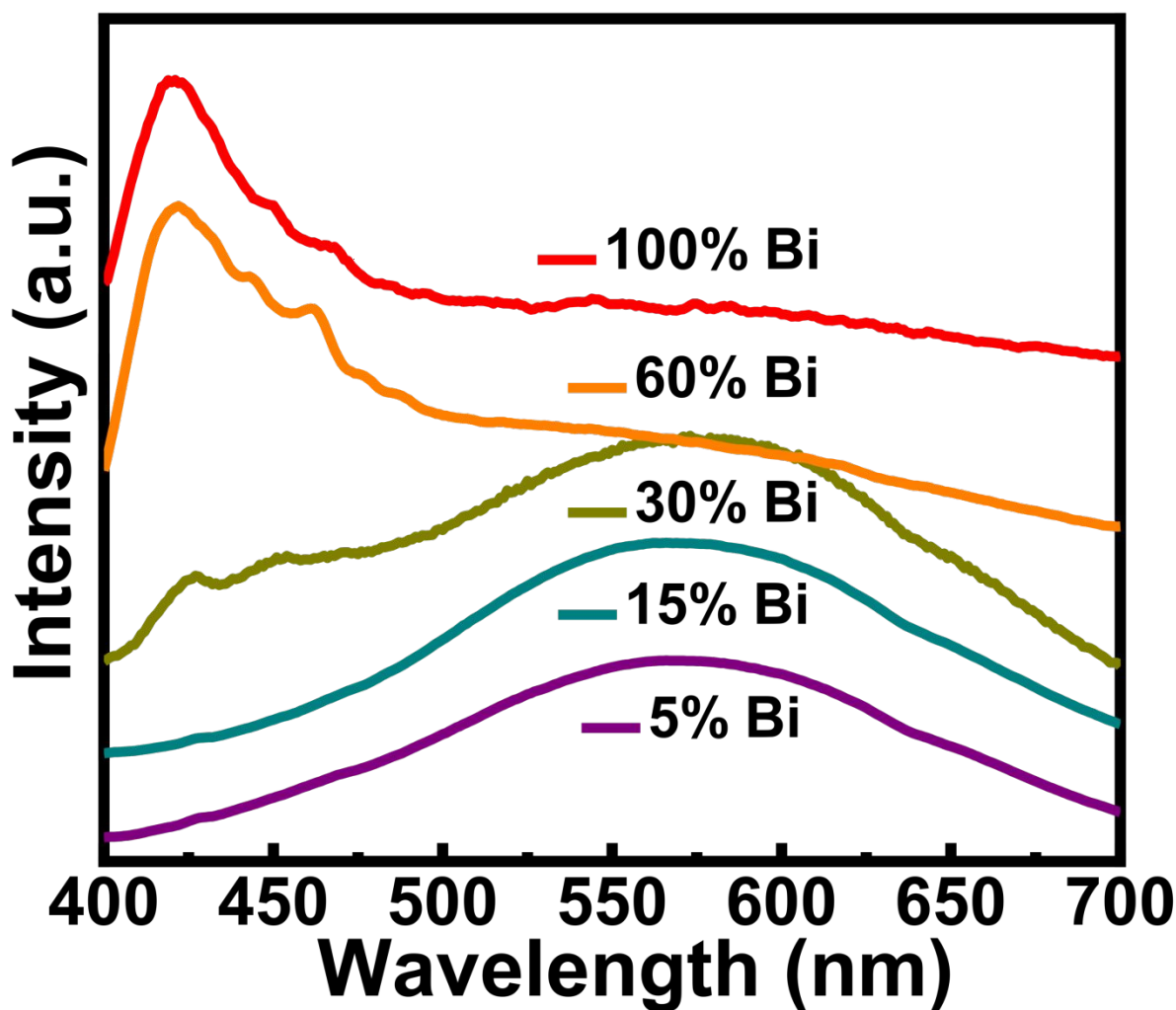


Figure S10. The PL spectra of $\text{Cs}_2\text{AgIn}_{1-x}\text{Bi}_x\text{Cl}_6$ ($x=0.05, 0.15, 0.3, 0.6$ and 1) double perovskites nanocrystals, collected at excitation source of 380 nm laser sources after three months of synthesis to study the stability of nanocrystals.

Table S1. Structural parameters estimated from the Rietveld refinements of XRD patterns of all the nanocrystal samples.

$\text{Cs}_2\text{AgIn}_{1-x}\text{Bi}_x\text{Cl}_6$	$x=0$	$x=0.05$	$x=0.15$	$x=0.3$	$x=0.6$	$x=100$
Crystal system	Cubic,	Cubic,	Cubic,	Cubic,	Cubic,	Cubic,
Space group	F m-3m	F m-3m	F m-3m	F m-3m	F m-3m	F m-3m
a , Å	10.4817	10.5015	10.5136	10.5566	10.6395	10.7742

b, Å	10.4817	10.5015	10.5136	10.5566	10.6395	10.7742
c, Å	10.4817	10.5015	10.5136	10.5566	10.6395	10.7742
V/ 10 ⁶ pm ³	1151.5	1163.4	1162.1	1176.4	1204.4	1250.73
Crystallite size (nm)	15	15	14	13	11	10
Goodness of fit	4.9	2.3	1.89	4.8	5.2	4.1

Table S2. Average nanocrystal size estimated from TEM, relative oscillator strength from UV-Vis absorption spectra, average life time estimated from TRPL, the bandgap of double perovskite nanocrystals from DRS and the quantum yield (QY) at defect level position at 580 nm with different doping concentration of Bi.

Cs ₂ AgIn _{1-x} Bi _x Cl ₆	x=0	x=0.05	x=0.15	x=0.3	x=0.6	x=100
Nanocrystal size, TEM (nm)	14.6	13.3	14.2	10.9	11	8
Relative oscillator strength	1	1.9	2.1	5.9	6.6	6.5
Av. Lifetime (ns)	--	11.3	7.5	12.8	17.3	--
Indirect bandgap (eV)	--	--	--	2.87/2.9	2.82/3.12	2.5/3.25
Direct bandgap (eV)	3.46	3.28	3.22	--	--	--
QY (%)	--	9.7	8.3	3.9		

Table S3. Compositional result of Cs₂AgIn_{1-x}Bi_xCl₆ double perovskites nanocrystals from STEM-EDS, SEM-EDS and XPS spectral analysis.

Cs ₂ AgIn _{1-x} Bi _x Cl ₆		x=0	x=0.05	x=0.15	x=0.3	x=0.6	x=100
STEM	Cs	26.16	24.61	29.22	27.01		29.16
	Ag	10.09	11.83	10.6	12.97		14.48
	In	14.38	10.31	12.91	9.61		00
	Bi	00	1.38	1.8	3.72		16.7
	Cl	49.37	51.88	45.47	46.69		39.66
		x=0	x=0.05	x=0.15	x=0.3	x=0.6	x=100
SEM	Cs	19.56	19.26	19.46	18.37	18.68	18.16
	Ag	9.92	10.51	10.41	9.77	9.95	10.04
	In	10.67	10.71	10.03	7.63	4.84	00

	Bi	00	1.15	1.37	2.63	5.18	10.45
	Cl	59.85	58.37	58.74	61.25	61.35	61.34
	Cs ₂ AgIn _{1-x} Bi _x Cl ₆	x=0	x=0.05	x=0.15	x=0.3	x=0.6	x=100
	Cs 3d	17.48	18.23	18.34	18.15	18.23	18.87
XPS	Ag 3d	9.29	9.89	8.45	9.78	9.28	9.65
	In 3d	13.01	10.23	11.54	9.33	6.69	00
	Bi 4f	00	1.78	2.81	3.76	5.20	11.46
	Cl 2p	60.22	60.1	58.86	58.99	60.59	60.01